International Journal of Engineering Inventions
e-ISSN: 2278-7461, p-ISSN: 2319-6491
Volume 12, Issue 6 [June. 2023] PP: 110-116

Numerical study on the temperature distribution of Lithium – Ion Battery

Nguyen Thanh Thuy[1], Nguyen Thi Thuy Hang[2*]
[1,2]Faculty of automotive and power machinery engineering, Thai Nguyen University of Technology, Thai Nguyen, Vietnam

ABSTRACT:
Lithium-ion batteries are widely used in Hybrid Electric Vehicles (HEVs) and Electrical Vehicles (EVs). However, the main drawback of the Lithium-ion batteries is that they generate a lot of heat due to ohmic and entropic reactions during charge/discharge. This increasing temperature during charge/discharge of HEVs and EVs may cause thermal runaway which can lead to a potential factor of igniting a very dangerous explosion and irreparable human injuries. Therefore, understanding the thermal behavior and discharge performance of Li-ion battery becomes even more necessary. In this study, the thermal behaviors of pouch type Lithium-Ion Batteries different discharge rates based on numerical simulations. The numerical simulation was performed via ANSYS Fluent traditional software package which utilizes the dual potential multi-scale multi-dimensional (MSMD) battery model to analyze the cell discharge behavior and investigate its thermal performance. The results showed that the maximum temperature of battery surface is proportional to the battery discharge rate, i.e., the higher the C-rate, the greater the cell surface temperature. The maximum temperature at discharge rates of 0.5C, 1 C, 2 C, and 3 C are respectively 301.70K, 307.60K, 326.30K and 362.20K which present 0.57%, 2.5%, 8.8% and 20.7% of temperature rise, respectively. Furthermore, it has been observed that the obtained model can be used in the design of a cooling system to eliminate non-uniform heat dissipation.
KEYWORDS: *Lithium-ion battery; thermal modelling; heat generation; Pouch type; Battery modelling, Heat distribution.*

Date of Submission: 02-06-2023 Date of acceptance: 12-06-2023

I. INTRODUCTION

The rapid expansion of the global population and continuous economic growth has resulted in a substantial surge in energy demand, which is projected to increase by 49% by 2030 [1]. Fossil fuels, such as coal, oil, and natural gas, have served as the primary energy source worldwide for hundreds of years. Developed over millions of years from organic matter, these finite resources have fueled global economic progress over the past century. However, as the demand for fossil fuels continues to rise steadily, their prices have escalated due to their limited availability. This issue is particularly critical in the transportation sector, a vital component of the global economy. The majority of transportation relies on internal combustion engines powered by fossil fuel oil, as alternative energy sources have yet to be fully developed for this purpose [2,3]. The use of fossil fuels is detrimental to the environment due to the emission of greenhouse gases (GHGs), contributing to global warming that affects all regions of the world [4,5]. Notably, the transportation sector stands as one of the largest contributors to GHG emissions, responsible for approximately one-third of the total emissions in the U.S. [6]. Therefore, the development of green vehicles such as hybrid electric vehicles (HEVs), battery electric vehicles (BEVs) and fuel cell electric vehicles (FCEVs) to reduce GHG emissions to allowable levels is one of the main research directions in the world [7].

One of the most favorable power sources for the above electric vehicles is a Lithium-ion battery with a long life cycle, safety and high durability. The lithium batteries contain lithium metal in their negative electrode. Currently, Li transition compounds such as LiCoO2, LiNiO2, LiMn2O4 and LiFePO4 are used as cathode material in battery cell production, and they have shown a good performance during charge and discharge cycling. However, the main drawback of the Lithium-ion batteries is that they generate a lot of heat due to ohmic and entropic reactions during charge/discharge [8]. This increasing temperature during charge/discharge of HEVs and EVs may cause thermal runaway which can lead to a potential factor of igniting a very dangerous

explosion and irreparable human injuries [9]. Therefore, understanding the thermal behavior and discharge performance of Li-ion battery becomes even more necessary.

In recent years, many investigations have been performed based on the modeling of lithium ion batteries. Nicolas et al. [10] studied on thermal modeling of large prismatic LiFePO4/graphite battery; coupled thermal and heat generation models for characterization and simulation. They proposed a parameter determination method based on a quasi-steady state assumption. Their approach considered the battery heating during characterization which is the temperature variation due to heat generation during current pulses. This temperature variation is estimated by combining of the coupled thermal and heat generation models. The electrical parameters are determined as a function of state of charge (SoC), temperature and current. Finally, they experimentally studied to validate their model with a precision of 10C. Lundgren et al. [11] showed a detailed 3D electrochemical-thermal model with experimental validation of a prismatic cell. Pals et al. [12] presented a one-dimensional model for predicting the thermal behavior of the lithium polymer battery. The simplified one-dimensional thermal modeling with lumped parameters was presented by Hallaj et al. [13] and others to simulate the temperature distribution inside lithium-ion battery cells. A multi scale multi-dimensional thermos-electrochemical modelling was proposed by Tourani el al. [14] to study the thermal behavior of lithium-ion cells.

The goal of this study is to determine the thermal behaviors of pouch type lithium ion battery at discharge rates of 0.5C, 1 C, 2 C, and 3 C. An electrical ECM model in ANSYS Fluent was employed. The results showed that the maximum temperature of battery surface is proportional to the battery discharge rate, i.e., the higher the C-rate, the greater the cell surface temperature. The maximum temperature at discharge rates of 0.5C, 1 C, 2 C, and 3 C are respectively 301.70K, 307.60K, 326.30K and 362.20K. Furthermore, it has been observed that the obtained model can be used in the design of a cooling system to eliminate non-uniform heat dissipation.

II. COMPUTATIONAL DOMAIN AND GOVERNING EQUATIONS

The dimensions of the calculation model of 14.6 Ah Lithium-ion battery which is simulated in the package software program are presented in Fig. 1a. The computational domain of Lithium battery is discretized using structured hexahedral mesh elements in Fig. 1b.

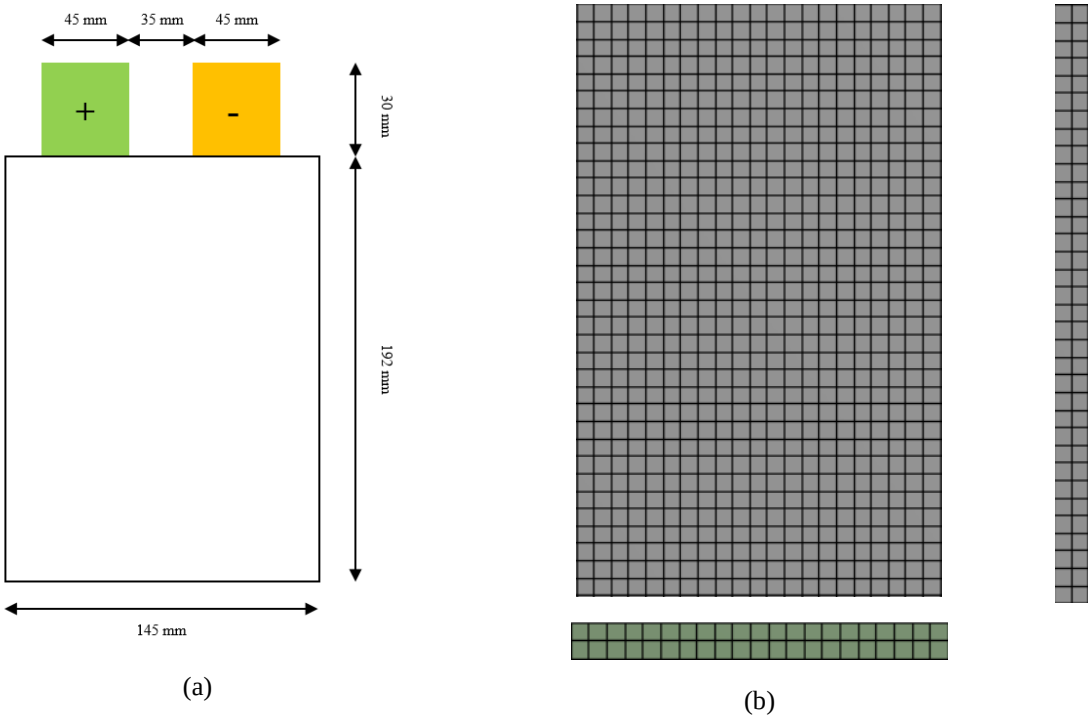

Figure 1: (a) Schematic of Lithium-ion battery cell applied in the simulation (the thichness is 2 mm) and (b) 3D meshing of 14.6 Ah Lithium-ion battery cell

In this study, a multi-dimensional (MSMD) approach was adopted and used, and this approach is described in [15]. It is built in ANSYS Fluent as MSMD battery model. It is important to note that MSMD method contains three electrochemical sub-models as following:

a) The Newman, Tiedemann, Gu and Kim models (known as NTGK);

b) Equivalent circuit model (Known as ECM).

c) Newman's Pseudo 2D model (known as Newman's P2D model).

In this work, an electrical ECM model is used because this approach represents a sufficient accuracy for thermal questions with at the same time acceptable computing time. The model uses the framework of the MSMD battery model architecture. The following mathematical differential equations are solved when applying the ECM model:

$$\frac{\partial_\rho C_p.T}{\partial t} - \nabla[k.\nabla T] = \dot{q}_{ECh} + \dot{q}_{Ohm} \quad (1)$$

$$\nabla\left[\sigma_+.\nabla\phi_+\right] = -j_{ECh} \quad (2)$$

$$\nabla\left[\sigma_-.\nabla\phi_-\right] = j_{ECh} \quad (3)$$

where (1) represents the spatial energy balance in the active material called jelly roll, the heart of lithium-ion cell where the electrochemic reactions and the heat generation take place. The internal energy is calculated by jelly roll's density ρ, specific heat capacity C_p, and temperature T. The spatial heat conduction is expressed with heat transfer coefficient k. $\dot{q}_{Ohm}$ is the heat generation from ohmic losses of the current collector foils of copper/aluminium in the jelly roll. $\dot{q}_{ECh}$ is the reaction heat from the electrochemical processes taking place such as charge transfer over potentials at the interface, and mass transfer limitations. Equations (2) and (3) are potential equations that describe the electrical behaviour. In these equations f is the phase potential, j_{ECh} the volumetric current transfer rate, and σ the electrical conductivity of the materials [1].

Using an ECM for the electrical modelling of the cell's behavior, the voltage is represented by:

$$U(t) = U_{OCV}(SOC,T) - U_{serial}(SOC,T) - U_{RC}(SOC,T) \quad (4)$$

whereat the voltage U is calculated in the ECM sub-model by the open circuit voltage UOCV and the voltage drop at the serial resistance Userial and the RC-element URC. All used parameters depend on local temperature and state of charge (SOC) in the jelly roll.

The electrochemical reaction heat is calculated from the equation below:

$$\dot{q}_{ECh} = j[U - U_{OCV}(SOC,T)] + j.T.\frac{dU_{OCV}}{dT}(SOC) \quad (5)$$

The first term considers the power loss due to the voltage drop at the internal resistance of the cell. The voltage U below is calculated in the ECM sub-model, the open-circuit voltage UOCV is part of the parameter set and the local current j results from the solution of the potential equations. This first part of the overall heat generation is irreversible. The second term considers the reversible heat generation based on an entropy change of the chemical system. This represents the reversible heat generation when multiplied with the local temperature T and the current j. Finally, the local heat generation is transferred in the 3D thermal model. The heat source changes temperatures, and therefore electrical resistances and heat generation, for the calculation of the next time step.

The default parameters used in ECM model are shown in Table 1. The study was used to obtain the discharge curves parameters of the typical 3.7 V lithium ion battery. Given that the ECM model adjusts the capacity of the modeled battery cell, it is found that the default parameters for this research are sufficient.

Table 1. MSMD Battery module input parameters

Parameter	Value	Units
Electrical parameters		
Nominal Cell Capacity	14.6	Ah
C-rate	0.5, 1, 2, 3	
Min. Stopping voltage	3	
Max. Stopping voltage	4.3	
Cell materials		
Density	2092	Kg/m^3
Specific Heat (C_p)	871	J/kg-K
Thermal conductivity	202.4	w/m-K
UDS-0	1.19e+06	Kg/m-s
UDS-1	9.83e+05	Kg/m-s
Electrical conductivity	3.541e+07	Siemens/m
Pole materials		
Density	8978	Kg/m^3
Specific Heat (C_p)	381	J/kg-K
Thermal conductivity	387.6	w/m-K
UDS-0	Model parameters	
Electrical conductivity	1e+07	Siemens/m

III.RESULTS AND DISCUSSION

The following figures will present the temperature and voltage variations during battery discharge.

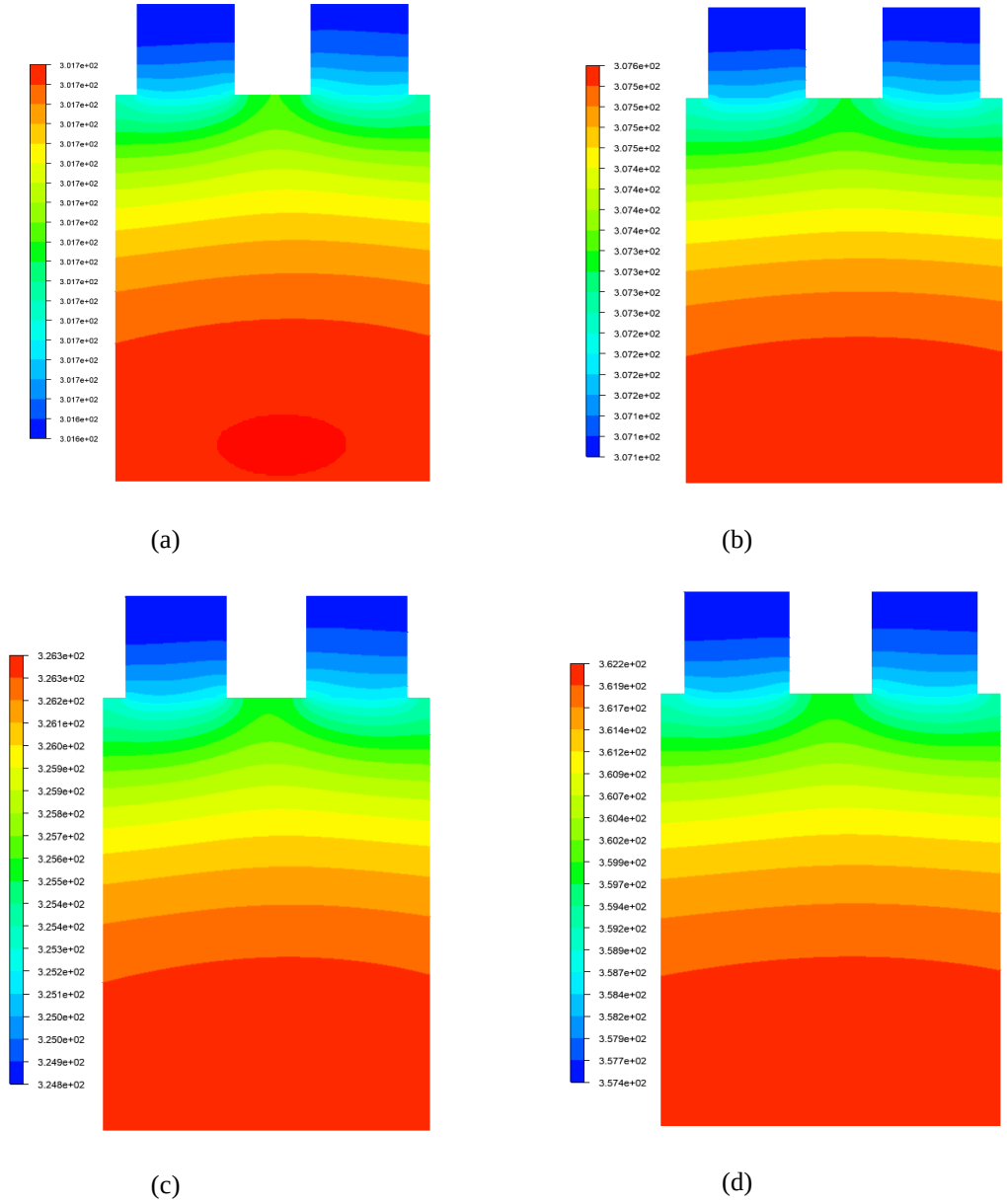

Figure 2. Temperature distributions at a) 0.5 C, b) 1 C, c) 2 C, d) 3C discharge rates

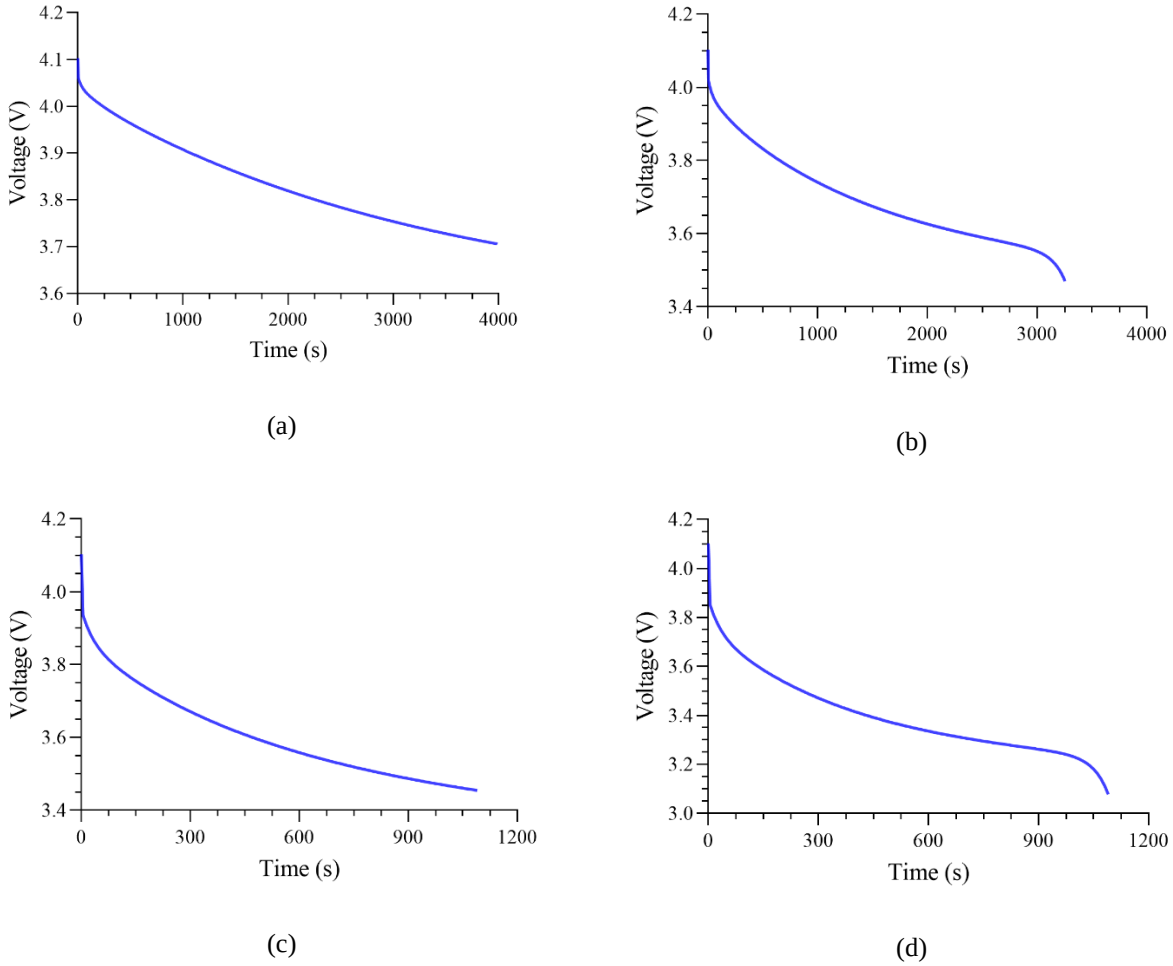

Figure 3. Discharge curves at a) 0.5 C, b) 1 C, c) 2 C, d) 3 C discharge rates

The discharge velocity parameters were applied as 0.5 C, 1 C, 2 C and 3 C, respectively. The ECM model parameters are the default parameters for the model of ANSYS Fluent. Material information has been entered into the system as cell material and polar material. Although polar materials are chosen differently for positive and negative materials some studies, this study has been chosen the same for does not make a big difference. Since the boundary conditions are very small in the extremes of the poles, it is assumed that there is no heat loss. The boundary conditions for poles and cells were taken from the ambient temperature 300 K and the heat transfer coefficient (h) 5 w/m^2K.

Figure 2 shows the temperature distributions in the discharge rates of 0.5 C, 1 C, 2 C and 3 C respectively. It can be seen that the temperature increases gradually depending on the discharge rates. As illustrated in this figure, the maximum battery cell surface temperature becomes 301.7^0K, 307.6^0K, 326.3^0K and 362.2^0K for 0.5 C, 1C, 2C, 3C discharge rate which present 0.57%, 2.5%, 8.8% and 20.7% of temperature rise, respectively. While the maximum temperature of cell has increased about 18.7 degrees for 2C in comparison with 1C, the maximum temperature of cell has increased about 35.9 degrees for 3C in comparison with 2C. The maximum cell surface temperature has reached 362.2^0 K which represents 62.2 degrees of increase incomparison with the battery temperature at the beginning of the simulation (300^0K). It becomes clearthat the influence of high C-rates on maximumtemperature is more than its impact at moderate or low C levels.

Figure 3 shows discharge curves in the discharge rates of 0.5C, 1C, 2C, and 3C respectively. As the discharge rate increases, the discharge time in the battery has been decreased. At the 0.5 C discharge rate, the battery voltage was considered to be 4.3V at the beginning and after 4000 seconds, it is predicted to be 3.7V.

This illustrate that the battery voltage has been reduced by 0.9V, i. e., 20.9 percentage of decrease. At 1 C, discharge rate battery voltage dropped from 4.3 V to 3.50 V in same time in 0.5C. However, at 2 C discharge rate battery voltage decrease from 4.3 V to 3.4 V in 1090 seconds, at 3 C discharge rate battery voltage decrease up to 3.07 V in same time in 2C.

V. CONCLUSION

A numerical study was conducted to determine thermal behavior of lithium-ion battery at different discharge rate of 0.5 C, 1 C, 2C, and 3C. The main conclusions of this work can be summarized as follows.

- The maximum temperature of battery surface is proportional to the battery discharge rate, i.e., the higher the C-rate, the greater the cell surface temperature.
- The maximum temperature at discharge rates of 0.5C, 1 C, 2 C, and 3 C are respectively 301.7^0K, 307.6^0K, 326.3^0K and 362.2^0K discharge rate which present 0.57%, 2.5%, 8.8% and 20.7% of temperature rise respectively.
- Furthermore, non-uniform thermal distribution has been observed when the discharge rate is increased. Non-uniform thermal distribution causes loss of capacity and performance in the battery. Therefore, an accurate and effective cooling system is required to eliminate non-uniform temperature distribution. These result are a preliminary preparation for cooling system design.

Acknowledgment

The authors would like to express our gratitude to the Thai Nguyen University of Technology for support of this work.

REFERENCES

[1]. Foley, P. M., Beach, E. S., and Zimmerman, J. B., 2011, "Algae as a Source of Renewable Chemicals: Opportunities and Challenges," Green Chem., **13**(6), p. 1399.
[2]. Mata, T. M., Martins, A. A., and Caetano, Nidia. S., 2010, "Microalgae for Biodiesel Production and Other Applications: A Review," Renewable and Sustainable Energy Reviews, **14**(1), pp. 217–232.
[3]. Reitz, R. D., Ogawa, H., Payri, R., Fansler, T., Kokjohn, S., Moriyoshi, Y., Agarwal, A., Arcoumanis, D., Assanis, D., Bae, C., Boulouchos, K., Canakci, M., Curran, S., Denbratt, I., Gavaises, M., Guenthner, M., Hasse, C., Huang, Z., Ishiyama, T., Johansson, B., Johnson, T., Kalghatgi, G., Koike, M., Kong, S., Leipertz, A., Miles, P., Novella, R., Onorati, A., Richter, M., Shuai, S., Siebers, D., Su, W., Trujillo, M., Uchida, N., Vaglieco, B. M., Wagner, R., and Zhao, H., 2020, "IJER Editorial: The Future of the Internal Combustion Engine," International Journal of Engine Research, **21**(1), pp. 3–10.
[4]. Hannon, M., Gimpel, J., Tran, M., Rasala, B., and Mayfield, S., 2010, "Biofuels from Algae: Challenges and Potential," Biofuels, **1**(5), pp. 763–784.
[5]. Bayro-Kaiser, V., and Nelson, N., 2017, "Microalgal Hydrogen Production: Prospects of an Essential Technology for a Clean and Sustainable Energy Economy," Photosynth Res, **133**(1–3), pp. 49–62.
[6]. United States Environmental Protection Agency, 2021, "Sources of Greenhouse Gas Emissions" [Online]. Available: https://www.epa.gov/ghgemissions/sources-greenhouse-gas-emissions. [Accessed: 26-Feb-2021].
[7]. Chen, Y., and Evans, J. W., 1993, "Heat Transfer Phenomena in Lithium/Polymer- Electrolyte Batteries for Electric Vehicle Application," J. Electrochem. Soc., **140**(7), pp. 1833–1838.
[8]. Chen, S. C., Wan, C. C., and Wang, Y. Y., 2005, "Thermal Analysis of Lithium-Ion Batteries," Journal of Power Sources, **140**(1), pp. 111–124.
[9]. Gu, W. B., and Wang, C. Y., 2000, "Thermal-Electrochemical Modeling of Battery Systems," J. Electrochem. Soc., **147**(8), p. 2910.
[10]. Damay, N., Forgez, C., Bichat, M.-P., and Friedrich, G., 2015, "Thermal Modeling of Large Prismatic LiFePO 4 /Graphite Battery. Coupled Thermal and Heat Generation Models for Characterization and Simulation," Journal of Power Sources, **283**, pp. 37–45.
[11]. Lundgren, H., Svens, P., Ekström, H., Tengstedt, C., Lindström, J., Behm, M., and Lindbergh, G., 2016, "Thermal Management of Large-Format Prismatic Lithium-Ion Battery in PHEV Application," J. Electrochem. Soc., **163**(2), pp. A309–A317.
[12]. Pals, C. R., and Newman, J., 1995, "Thermal Modeling of the Lithium/PolymerBattery," J. Electrochem. Soc., **142**(10).
[13]. Hallaj, S. A., Maleki, H., Hong, J. S., and Selman, J. R., 1999, "Thermal Modeling and Design Considerations of Lithium-Ion Batteries."
[14]. Tourani, A., White, P., and Ivey, P., 2014, "A Multi Scale Multi-Dimensional Thermo Electrochemical Modelling of High Capacity Lithium-Ion Cells," Journal of Power Sources, **255**, pp. 360–367.
[15]. Kim, G.-H., Smith, K., Lee, K.-J., Santhanagopalan, S., and Pesaran, A., 2011, "Multi-Domain Modeling of Lithium-Ion Batteries Encompassing Multi-Physics in Varied Length Scales," J. Electrochem. Soc., **158**(8), p. A955.
[16]. Kleiner, J., Komsiyska, L., Elger, G., and Endisch, C., 2019, "Thermal Modelling of a Prismatic Lithium-Ion Cell in a Battery Electric Vehicle Environment: Influences of the Experimental Validation Setup," Energies, **13**(1), p. 62.